

Evaluation of $y(\text{UTC}(\text{NICT}))$ with respect to NICT-Sr1 for the period MJD 59514 to 59534

We have evaluated the fractional frequency deviation of the time scale $\text{UTC}(\text{NICT})$ for the period from MJD 59514 to 59534 (Oct. 27 – Nov. 16 in 2021) to be $\overline{y(\text{UTC}(\text{NICT}))} = -6.06 \times 10^{-16}$, using secondary frequency standard NICT-Sr1.

NICT-Sr1 measured the mean frequency deviation frequency of hydrogen maser $\text{HM}_{1402014}$ to be $\overline{y(\text{HM}_{1402014})} = -2.1228 \times 10^{-14}$, and the frequency of $\text{UTC}(\text{NICT})$ was then determined by using NICT's Japan Standard Time system.

The optical lattice clock acquired data for 43 351 s (2.5% of the total evaluation period) over three operating intervals on MJD 59516, 59523 and 59530, as shown in Fig. 1. The resulting uncertainties are represented in the following table according to Circular T notation:

Period of Estimation (MJD)	$\overline{y(\text{UTC}(\text{NICT}))}$	u_A	u_B	$u_{A/\text{Lab}}$	$u_{B/\text{Lab}}$	u_{Srep}	uptime
59514 – 59534	-6.06	0.34	0.69	2.17	0.80	4	2.5%
Effect	Uncertainty	u_A	u_B				
$u_{A/\text{Sr}}$	0.34	✓					
u_B	0.69		✓				
HM: linear trend estimation	1.77			✓			
HM: stochastic noise	1.26			✓			
Optical-microwave comparison / microwave transfer	0.80				✓		
Uncertainty of Sr as SRS	4					✓	

Table 1. Results of evaluation. All number are in parts of 10^{-16} .

The evaluation employs the recommended value of the ^{87}Sr clock transition as a secondary representation of the second: $\nu(^{87}\text{Sr}) = 429\,228\,004\,229\,873.0$ Hz with its relative standard uncertainty of $u_{\text{Srep}} = 4 \times 10^{-16}$, determined by the 21st CCTF in June 2017.

u_A is the Type A uncertainty of NICT-Sr1 as an optical standard. It represents the statistical uncertainty determined by interleaved measurements [1].

u_B is the Type B uncertainty of NICT-Sr1 [1 – 3], including the uncertainty of the gravitational redshift.

$u_{A/\text{Lab}}$ and $u_{B/\text{Lab}}$ represent the uncertainty due to the link between NICT-Sr1 and the HM [2, 3]. They consist of

Type B uncertainty $u_{B/\text{Lab}} = 7.95 \times 10^{-17}$ due to the frequency comparison between microwave and optical signals, including distribution of the microwave signals, and

Type A uncertainty $u_{A/\text{Lab}} = 2.17 \times 10^{-16}$ representing the linear trend estimation of the HM ($u_{1/\text{trend}}$), the uncertainty due to the stochastic noise of the HM during unobserved intervals ($u_{1/\text{stoch}}$).

1. Evaluation of the frequency of hydrogen maser $\text{HM}_{1402014}$ with respect to NICT-Sr1 over 20 days

The details of NICT-Sr1 are described in [1, 2]. The Sr atoms were laser-cooled using a two-stage laser cooling technique and loaded to a vertically oriented one-dimensional optical lattice.

We transfer the HM behavior to an Er:fiber comb by stabilizing a heterodyne beat between the 37th harmonic of the frequency comb's approximately 250 MHz repetition rate and a 9.3 GHz signal from a dielectric resonator oscillator phase-locked to the 100 MHz signal of $\text{HM}_{1402014}$. The optical frequency reference at 698 nm supplied by NICT-Sr1 is measured as a beat with a frequency-doubled output branch of the comb. The comb repetition rate is detected at the output of the same output branch to reduce variations in relative phase, and the system incorporates a temperature-stabilized baseplate to maintain stable optical path lengths. The phase-locked beat signals for carrier-envelope offset and repetition rate are monitored by zero-deadtime counters.

The frequency comb system used in previous measurements operates simultaneously to confirm the measurement results. In this system, the repetition rate is stabilized by phase-lock of the heterodyne beat between the 82nd harmonic of the frequency comb's approximately 100 MHz repetition rate and an 8.2 GHz dielectric resonator oscillator phase-locked to the 100 MHz signal of $\text{HM}_{1402014}$. A transfer laser at 1397 nm is frequency-doubled by a PPLN waveguide. Its output is separated into a visible component used to phase-lock the laser to the optical frequency reference at 698 nm supplied by NICT-Sr1, and a residual infrared component that generates a beat signal with the frequency comb. This beat is counted both directly and through a tracking oscillator to allow rejection of cycle slips.

Both comb systems show agreement at a level below their statistical uncertainties.

The fractional deviation of the HM frequency from its nominal value is stored pre-averaged in 10 s bins. Weights are assigned according to the number of contributing data points in each bin.

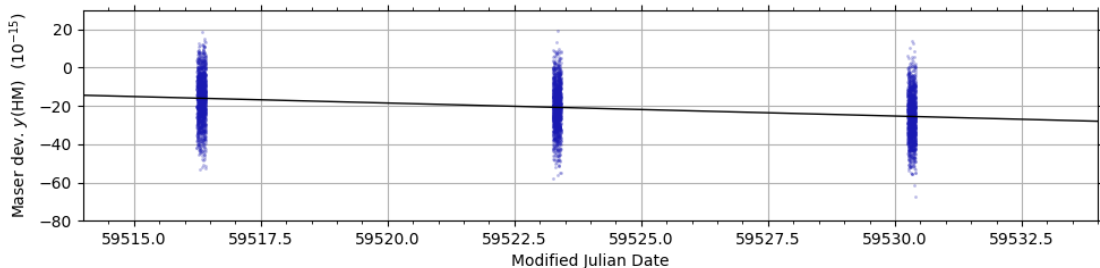


Fig.1. Distribution of maser frequency measurements in terms of fractional deviation $y(\text{HM})$ from the nominal frequency. The black solid line indicates the linear fit used to obtain the mean value over the evaluation interval.

2. Treatment of stochastic noise during unobserved intervals

For intermittent clock operation, phase and frequency excursions of the HM during unobserved intervals contribute significant measurement uncertainty [2, 4].

To mitigate their overall effect, we include a total of three HMs in the evaluation ($\text{HM}_{1402003}$, $\text{HM}_{1402004}$ and $\text{HM}_{1402014}$). Their relative phase is continuously monitored by the Japan Standard Time dual-mixer time-difference (DMTD) system. We calculate the frequency difference of each HM from the ensemble average and confirm the absence of abnormal behavior during the evaluation period. We then determine the frequency of $\text{HM}_{1402014}$ with respect to the ensemble. By subtracting frequency offset and linear trend from this relative frequency, we obtain residuals that approximate the instantaneous deviation of $\text{HM}_{1402014}$ from a pure linear drift, while summing to

zero over the evaluation period. We use these residuals (calculated for a set of one-hour intervals) to correct the HM frequency measured with respect to the Sr clock. The result is an improved representation of the mean frequency and linear drift of HM₁₄₀₂₀₁₄ over the complete evaluation period. A weighted linear fit is applied to the corrected data to find the frequency corresponding to the midpoint of the 20-day interval. The ensemble-based corrections result in a change of the reported HM frequency by -1.52×10^{-16} compared to the result obtained using only HM₁₄₀₂₀₁₄.

We characterize the typical instability of a single maser based on evaluation of several years of continuous data using three-corner-hat methods, and find that for large averaging times it is well-described by an Hadamard variance $\sigma_H^2(\tau) = a_{-1} + a_{-3} \tau^2$. Here, $a_{-1} = (2.1 \times 10^{-16})^2$ represents flicker frequency noise (FFN) [5] while the slow-varying noise that dominates the long-term instability through $a_{-3} = (1.9 \times 10^{-22}/s)^2$ is typically referred to as flicker-walk frequency modulation (FWFM) [6]. We follow the approach described in the supplement of ref. [7] to determine the uncertainty of extrapolating from the inhomogeneously distributed data to the full evaluation period. This yields a distribution-specific sensitivity to the HM's noise power spectral density (PSD) [7], which we obtain from the observed maser instabilities a_{-1} and a_{-3} through the relations

$$\text{FFN: } \sigma_H^2(\tau) = \frac{1}{2} \ln\left(\frac{256}{27}\right) h_{-1} \quad \text{for } S_y^{\text{FFN}} = h_{-1} f^{-1} \quad \text{and} \quad (1)$$

$$\text{FWFM: } \sigma_H^2(\tau) = \frac{16}{6} \pi \ln\left(\frac{3}{4} \cdot 3^{11/16}\right) h_{-3} \tau^2 \quad \text{for } S_y^{\text{FWFM}} = h_{-3} f^{-3} \quad , \quad (2)$$

according to refs. [6, 8]. Additional information on the procedure is available in ref. [4]. Despite the complexity of FFN and FWFM in the temporal domain, the noise can always be expressed as a sum over normally distributed sources, and there is no correlation between the noise encountered in separate masers. The maser ensemble therefore shows the same uncertainty reduction with $N_{\text{ens}}^{-1/2}$ as other noise types.

For the present (inhomogeneous) measurement distribution and PSDs, this leads to the uncertainty contributions $u_{1/\text{FFN}} = 1.23 \times 10^{-16}$ and $u_{1/\text{FWFM}} = 2.5 \times 10^{-17}$, which we include as $u_{1/\text{stoch}} = 1.26 \times 10^{-16}$.

3. Determination of statistical and systematic contributions to $u_{1/\text{Lab}}$

We determine a statistical uncertainty of the maser frequency measurement $u_{\text{stat}} = 1.71 \times 10^{-16}$ from the residuals of a linear fit by extrapolating the Allan deviation from the region limited by white frequency noise (30–2 000 s) to the full length of available data.

When plotting the instability of the frequency measurements for HM₁₄₀₂₀₁₄ in terms of the Hadamard deviation, we expect an observed flicker floor $\sigma_L^2 \approx a_{-1}$ due to FFN.

Since the barycenter of the data (approximately MJD 59525.40) differs from the midpoint (MJD 59524.0) of the evaluation period by +120 687 s, the uncertainty of the maser drift rate contributes an uncertainty of $u_{\text{drift}} = 4.4 \times 10^{-17}$, such that

$$u_{1/\text{trend}} = (u_{\text{stat}}^2 + u_{\text{drift}}^2)^{1/2} = 1.77 \times 10^{-16}.$$

While intermittent measurements of the maser frequency are easily affected by phase shifts resulting from thermalization effects at the start of frequency comb operation, as well as from diurnal temperature variation, an investigation of data obtained over a ten-day interval [9] sets a limit of $u_{\text{B,1}/\text{Lab}} = 7.95 \times 10^{-17}$ for the window of $T_{\text{typ}} = 21\,600$ s (6 h) duration during which intermittent measurements are typically performed. Frequency combs and measurement instruments are operated continuously to avoid start-up effects and maintain a constant heat load in the laboratory.

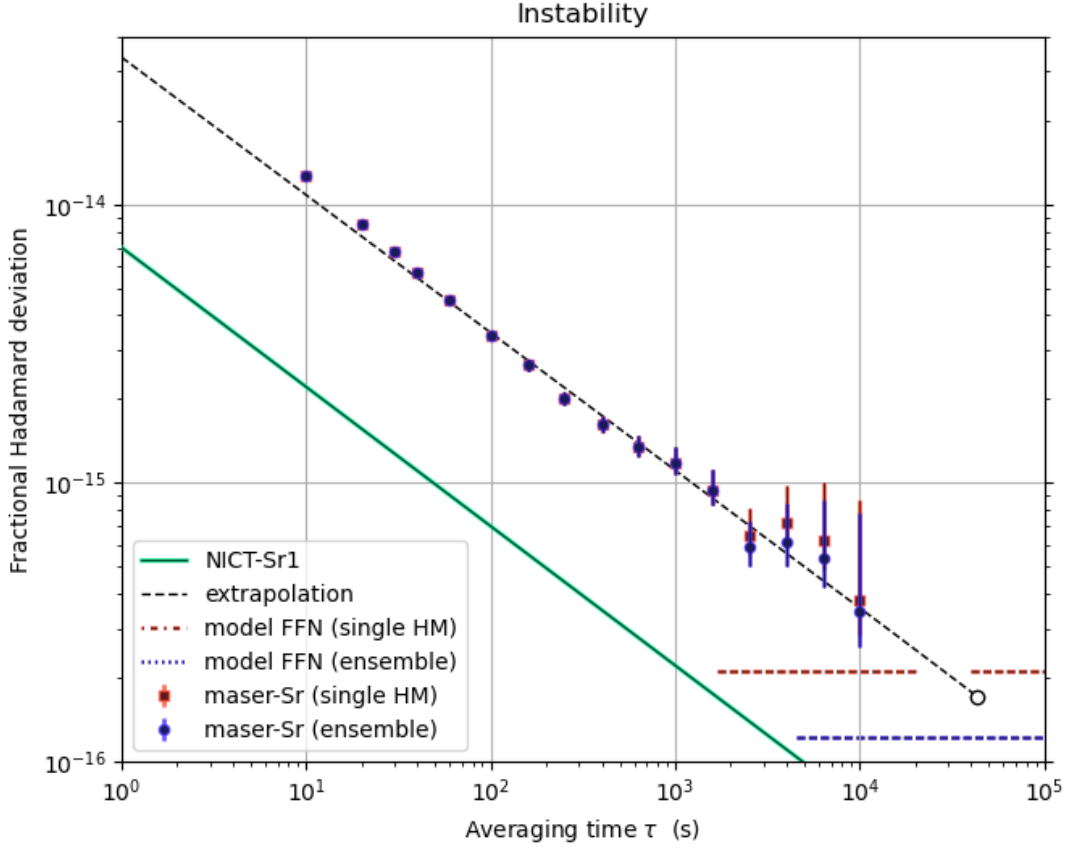


Fig.2. Instability of maser frequency measurements with respect to NICT-Sr1. Blue circles and red squares show the overlapping Hadamard deviation for the residuals from a linear fit with and without correction for deviation of the HM from linear drift, as determined using an ensemble of 3 HMs. Gaps have been removed by contracting the data into a continuous interval. Error bars indicate 1σ uncertainties, calculated for white frequency noise. The dashed line indicates the extrapolation to the full length of available data, used to obtain the statistical uncertainty indicated by the open mark. For long averaging times, the Hadamard deviation falls to a level consistent with the maser stability model, indicated by the red upper dashed line for a single maser, and by the blue lower dashed line for the ensemble, where the instability is expected to improve by a factor of $1/\sqrt{N_{\text{ens}}}$. The green line shows the instability contribution from NICT-Sr1.

4. Frequency deviation of UTC(NICT)

The frequency difference between $\text{HM}_{1402014}$ and UTC(NICT) over the evaluation period is calculated as

$$y(\text{UTC}(\text{NICT}) - \text{HM}_{1402014}) = (\delta_a - \delta_b)/T, \quad (3)$$

where δ_a and δ_b represent the time difference $\text{UTC}(\text{NICT}) - \text{HM}_{1402014}$ at the beginning and end of an evaluation interval of length T . These values are continuously measured by the DMTD system [10] and reported to BIPM, where they are used in the EAL generation and made available at <https://webtai.bipm.org/ftp/pub/tai/data/>. In addition to the DMTD system, the Japan Standard Time generation system also monitors all time differences by a time interval counter. Both measurements agree and show no sudden changes in the time differences or any other indication of measurement errors.

5. Accuracy of NICT-Sr1

The systematic corrections and their uncertainties for NICT-Sr1 [1 – 3] are summarized below:

Effect	Correction (10^{-17})	Uncertainty (10^{-17})
Blackbody radiation	508.6	2.6
Lattice scalar / tensor	0	5.3
Lattice hyperpolarizability	-0.2	0.1
Lattice E2/M1	0	0.5
Probe light	0.1	0.1
Dc Stark	0.1	0.2
Quadratic Zeeman	51.1	0.3
Density	0.7	0.5
Background gas collisions	0	1.8
Line pulling	0	0.1
Servo error	-3.2	1.9
Total	557.2	6.5
Gravitational redshift	-834.1	2.2
Total (with gravitational effect)	-276.9	6.9

Table 2. Systematic corrections and their uncertainties for NICT-Sr1.

6. References

- [1] H. Hachisu and T. Ido, “Intermittent optical frequency measurements to reduce the dead time uncertainty of frequency link,” *Jpn. J. Appl. Phys.* **54**, 112401 (2015).
- [2] H. Hachisu, G. Petit, F. Nakagawa, Y. Hanado and T. Ido, “SI-traceable measurement of an optical frequency at low 10^{-16} level without a local primary standard,” *Opt. Express* **25**, 8511 (2017).
- [3] H. Hachisu, F. Nakagawa, Y. Hanado and T. Ido, “Months-long real-time generation of a time scale based on an optical clock,” *Sci. Reports* **8**, 4243 (2018).
- [4] N. Nemitz *et al.*, “Absolute frequency of 87Sr at 1.8×10^{-16} uncertainty by reference to remote primary frequency standards,” *Metrologia* **58**, 025006 (2021)
- [5] D. Allan, “Time and frequency (time-domain) characterization, estimation, and prediction of precision clock and oscillators,” *IEEE UFFC* **34**, 647 (1987).
- [6] W. J. Riley, “Handbook of Frequency Stability Analysis,” NIST Special Publication 1065 (2008)
- [7] C. Grebing *et al.*, “Realization of a timescale with an accurate optical lattice clock,” *Optica* **3**, 563-569 (2016).
- [8] S.T. Dawkins, J. J. McFerran and A. Luiten, “Considerations on the Measurement of the Stability of Oscillators with Frequency Counters,” *IEEE Trans. UFFC* **54**, 918-925 (2007).
- [9] Evaluation report “nict-sr1_58454-58464 [January 2019],” available at <https://www.bipm.org/en/bipm-services/timescales/time-ftp/data.html>.
- [10] F. Nakagawa *et al.*, “Development of multichannel dual-mixer time difference system to generate UTC(NICT),” *IEEE Trans. Instrum. Meas.* **54**, 829 (2005).